

## Nanowire thermometers

Cite this: DOI: 10.1039/c3nr03086e

Peng Peng,<sup>a</sup> Zhihua Su,<sup>a</sup> Zhihong Liu,<sup>a</sup> Qingkai Yu,<sup>\*b</sup> Zhengdong Cheng<sup>\*c</sup>  
and Jiming Bao<sup>\*a</sup>

Received 15th June 2013

Accepted 14th August 2013

DOI: 10.1039/c3nr03086e

www.rsc.org/nanoscale

We report the design and demonstration of nanowire temperature reporters. Metal alloys with tunable melting points were used to create nanowires in nanopores of anodic aluminum oxide using mechanical pressure injection. When exposed to temperature above their melting points, nanowires began to break up into disconnected shorter nanorods due to Rayleigh instability. A wide range of temperature can be probed conveniently by measuring electrical resistance of nanowires.

There have been considerable efforts devoted to the development of nanometer scale thermometers.<sup>1</sup> A nanoscale temperature reporter is a special nanothermometer which can act as a stand-alone sensor and be deployed in circumstances with limited or no access for *in situ* temperature monitoring. Several such nanothermometers have recently been demonstrated.<sup>2–4</sup> Silver nanoparticle nanothermometers exploit the dependence of particle size on the exposed temperature.<sup>2</sup> Ga-filled carbon nanotube (CNT) thermometers rely on the oxide mark created by a thermally expanded gallium column in the CNT at the highest temperature.<sup>3</sup> The unique thermal dewetting properties of ultrathin Au films can also be used to provide a temperature fingerprint.<sup>4,5</sup> These temperature reporters utilize temperature-dependent irreversible morphological changes that can later be interrogated to provide temperature information and they function differently from other nanothermometers that utilize the reversible temperature-dependent physical properties such as fluorescence,<sup>6–8</sup> thermal expansion,<sup>9,10</sup> blackbody radiation<sup>11</sup> and electrical resistivity.<sup>12,13</sup>

In this communication, we demonstrate a new type of temperature reporters that utilize Rayleigh instability to create irreversible morphological changes to nanowires.<sup>14</sup> A straightforward fabrication technique was adopted to prepare and protect metallic nanowires in porous anodic aluminum oxide (AAO).<sup>15</sup> An important characteristic of nanowire temperature reporters is the melting point, above which nanowires become fragmented due to Rayleigh instability. Based on morphological or electrical changes of the nanowires, we can learn whether or not the nanowire sensors have been exposed to the predefined characteristic temperatures. Reporters with different characteristic temperatures can be fabricated using alloys with different melting points. Such alloys are commercially available and their melting points can be nearly continuously tuned from 42 to ~700 °C.<sup>16</sup> To demonstrate the concept, we choose indium (In) and one of its alloys as the material for nanowires.

Fig. 1(a) shows the method that we used to create In or In alloy nanowires inside AAO nanopores.<sup>15</sup> An indium (or indium alloy) foil is first placed on an AAO membrane surface; it is then pressed against the AAO membrane with a high mechanical pressure. A proper pressure and an elevated temperature (~20 °C below the melting point of indium or indium alloy) are applied in order to push indium to the other side of the AAO membrane, as shown in Fig. 1(b). Fig. 1(c) shows a scanning electron microscopy (SEM) image of long and continuous In nanowires after KOH dissolving of AAO.

The nanowires become fragmented when exposed to a temperature higher than their melting point, which can be clearly seen in Fig. 2. Because nanowires are encapsulated in the nanopores of the AAO membrane, SEM pictures are taken from the cross-section of the AAO membrane. Fig. 2(a) shows In nanowires located on the cleaved surface just behind AAO walls. More nanowires can be seen in Fig. 2(b) after the removal of AAO walls by KOH etching. In order to get a picture of the evolution of nanowire fragmentation, nanowires are imaged after exposure to different temperatures for 30 minutes. As can be seen in Fig. 3, In nanowires do not become fragmented until they are exposed to a temperature above the melting point. The

<sup>a</sup>Department of Electrical and Computer Engineering, University of Houston, Houston, TX 77204, USA. E-mail: jbao@uh.edu

<sup>b</sup>Ingram School of Engineering, and Materials Science, Engineering and Commercialization Program, Texas State University, San Marcos, TX 78666, USA. E-mail: qingkai.yu@txstate.edu

<sup>c</sup>Artie McFerrin Department of Chemical Engineering, Department of Materials Science and Engineering, Texas A&M University, College Station, TX 77843, USA. E-mail: zcheng@tamu.edu

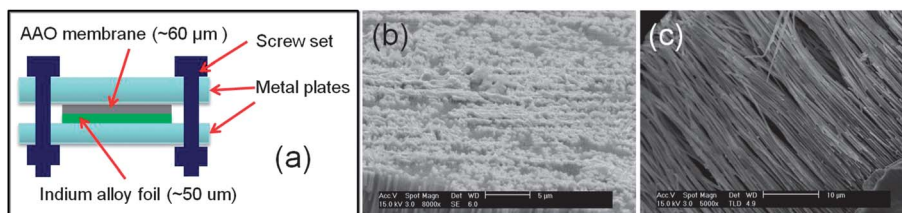


**Fig. 1** Fabrication of indium (In) nanowires using porous anodic aluminum oxide (AAO). (a) Schematic of a mechanical device that is used to inject In into AAO nanopores from one side of AAO membrane surfaces. (b) Scanning electron microscopy (SEM) image of the backside of the AAO membrane showing the emergence of In nanowires through AAO nanopores. (c) SEM picture of indium nanowires after AAO is dissolved by KOH chemical etching.

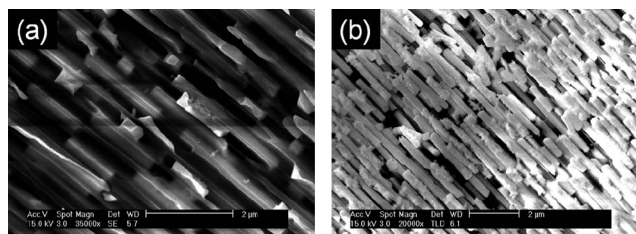


**Fig. 2** SEM images of fragmented In nanowires after annealing at 305 °C for 30 minutes. The melting point of In is 156 °C. (a) From a cleaved surface parallel to the nanowires. (b) After dissolving of AAO by KOH.

fragments become shorter at higher annealing temperatures. A similar result is observed with lower melting point InSn alloy nanowires, as shown in Fig. 4.

Nanowire resistance measurement was employed in order to investigate the fragmentation of nanowires without breaking the AAO membrane and nanowires, as well as to obtain a more quantitative indication of fragmentation near the nanowire melting points. Fig. 5(a) shows the schematic of the experimental setup where two probes were put in contact with the

opposite sides of the AAO membrane. Fig. 5(b) shows the results after annealing nanowires for 30 minutes at different temperatures. It can be seen that the initial resistance at room temperature was very small and that it stayed nearly the same when the annealing temperatures were kept below the nanowire melting points. But the resistance jumped abruptly once the annealing temperature rose above the melting points. The resistance rose sharply with increasing temperature until it began to saturate at about 30 degrees higher than the melting points. We also observed that the resistance increased with longer annealing time if the annealing temperature was fixed.

Rayleigh instability is responsible for the observed nanowire fragmentation, it states that liquid streams are not stable morphologically due to surface tension.<sup>14</sup> For example, if a liquid stream is not confined, it will break up and eventually becomes an array of spherical droplets that reduce surface energy. Rayleigh instability was later extended to explain similar morphological changes in solids,<sup>17</sup> and has been observed in many types of cylindrical nanostructures made of either metal or polymer.<sup>18–24</sup> The size and shape of fragmented nanostructures depend on the type of confinement and available

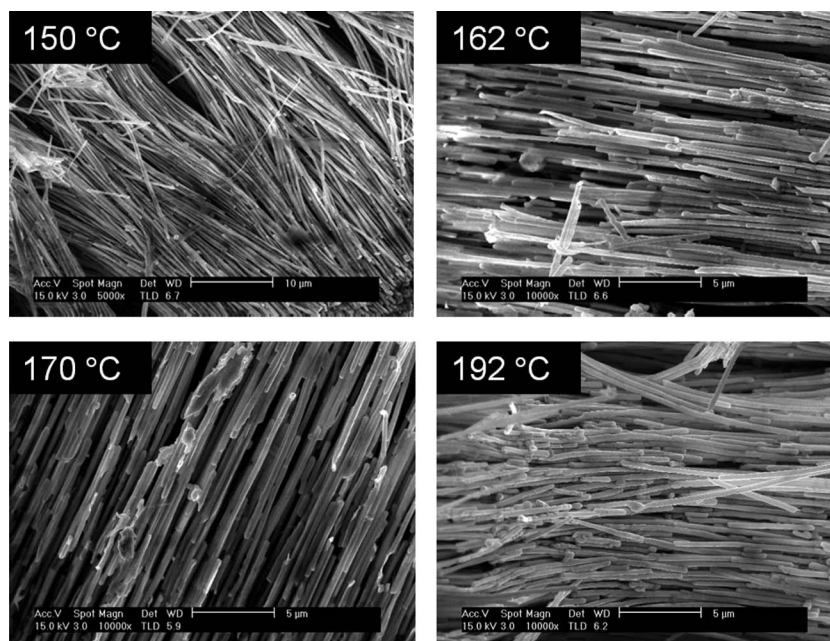


**Fig. 3** Fragmentation of In nanowires after 30 minutes of annealing at different temperatures below and above the 156 °C melting point of In.

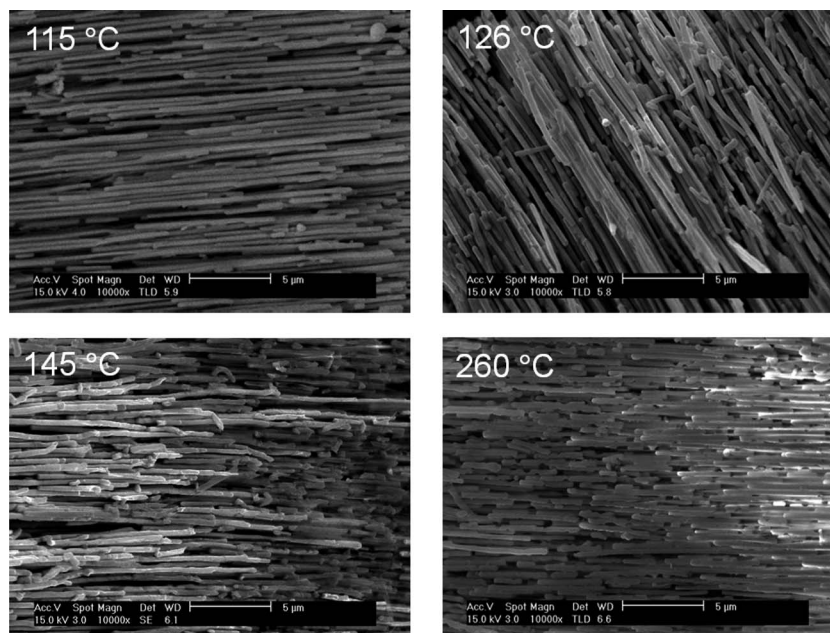


Fig. 4 Fragmentation of InSn alloy nanowires after 30 minutes of annealing at different temperatures below and above the melting point of InSn at 118 °C.

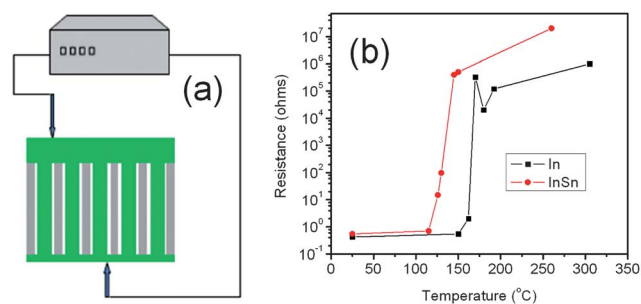


Fig. 5 Nanowire fragmentation probed by resistance measurement. (a) Schematic of experimental setup for measuring resistance of nanowires. Green represents indium alloy, and grey is AAO. (b) Increases of resistance of indium (black) and InSn (red) nanowires after annealing at different temperatures for 30 minutes. The uncertainty of temperature measurement above room temperature is  $\sim 3$  °C because of thermal fluctuation of the furnace when it was trying to stabilize to the desired points.

space. The rate of the morphological transformation is mainly determined by the viscosity, which depends on the temperature of the material. Due to the reduced viscosity, a higher temperature will accelerate the transformation. We believe that different distributions of fragmented nanowires shown in Fig. 2–5 exhibit intermediate states of morphological transformation.<sup>20,23</sup> The fragmentation becomes more complete at higher temperatures as shown in Fig. 2 and 4.

It is to be noted that the observed Raleigh instability was made possible by the way the nanowires were fabricated. Because In alloy was injected below the melting temperature, nanopores were not completely filled by the nanowires. Furthermore, it is expected that such fabricated nanowires will have a large density of structural defects, even large-size voids. Due to above reasons, unfilled space between fragments was

created once nanowires melted, providing a necessary condition for the Rayleigh instability.<sup>18,21</sup> Although nanowire fragmentation has been observed at temperatures much lower than the melting point of the bulk materials, but it will take longer time, and it happens to nanowires with diameter less than 30 nm.<sup>20,23</sup> The main reason why Rayleigh instability was only observed at the temperature slightly above the melting point in our case is the large diameter of  $\sim 350$  nm of our nanowires. These nanowires have almost the same melting point as the bulk material.<sup>24</sup> The confinement of nanowires inside AAO nanopores can also reduce the rate of morphological transformation of nanowires.<sup>21</sup> We believe that it will take from tens of hours to many days for the fragmentation of our nanowires to happen if the temperature is held far below the melting temperature (for instance, 10 °C below).

The melting point of nanowires and the onset of fragmentation provide the basis for temperature reporters. Because fragmentation will result in an abrupt increase in electrical resistance of a single nanowire, the relatively gradual increase of resistance near the melting points in Fig. 5(b) is due to the fact that the resistance is averaged over a large number of nanowires connected to the millimeter-size probes. Based on the resistance measurement and SEM imaging, such many-nanowire thermometers have a temperature resolution of 10 °C and a response time of 30 minutes. In order to maintain such temperature resolution, the exposure time should be limited to a few days because of possible nanowire fragmentation below the melting point. The temperature resolution can be improved if the thermometer is made of a single or a few nanowires. Because the diameter and length of AAO nanopores can be well controlled during the anodic processing and the AAO membrane can be cut into micro or nanometer size using modern lithographic techniques,<sup>25</sup> few-nanowire nanothermometers with improved



performance can be fabricated. Furthermore, by integrating nanothermometers with different threshold temperatures, more precise temperature information can be obtained. The choice of AAO has also made it possible to deploy the device in a harsh environment.

## Conclusions

To summarize, we have shown that morphological transformation of nanowires confined in nanopores can be utilized to make nanowire temperature reporters. The nanowire morphological transformation is driven by the Rayleigh instability. The characteristic temperature is determined by the nanowire melting point and can be designed by choosing proper nanowire alloys. Additional temperature information could also be obtained from intermediate states of morphological transformation. Because of the unique temperature reporting capability, the nanowire nanothermometers can allow us to obtain temperature information from locations that cannot be accessed by reversible nanothermometers. For example, a nanowire thermometer can be injected in a pipeline and drift with the fluid. When collected, it can tell us whether or not there is a “hot spot” along the pipeline. A nanowire temperature reporter can also function in almost the same way as a commercial temperature indicator WarmMark from ShockWatch except that a WarmMark is powered and has built-in electronics that can record the exposure time.<sup>26</sup> A WarmMark “alerts users of exposure to unacceptable temperature conditions”.<sup>26</sup> Likewise, a nanowire thermometer can be attached to or embedded in any subjects, and it can later indicate whether the subjects have been exposed to a temperature higher than the designed threshold.

## Acknowledgements

This work was supported by Advanced Energy Consortium (BEG10-03). J.M.B. acknowledges support from the Robert A Welch Foundation (E-1728). Q.Y. acknowledges DTRA Grant (HDTRA1-10-1-0002).

## Notes and references

- 1 J. Lee and N. A. Kotov, *Nano Today*, 2007, **2**, 48–51.
- 2 Y. C. Lan, H. Wang, X. Y. Chen, D. Z. Wang, G. Chen and Z. F. Ren, *Adv. Mater.*, 2009, **21**, 4839–4844.
- 3 Y. H. Gao, Y. Bando, Z. W. Liu, D. Golberg and H. Nakanishi, *Appl. Phys. Lett.*, 2003, **83**, 2913–2915.
- 4 H. T. Sun, M. P. Yu, X. Sun, G. K. Wang and J. Lian, *J. Phys. Chem. C*, 2013, **117**, 3366–3373.
- 5 H. T. Sun, M. P. Yu, G. K. Wang, X. Sun and J. Lian, *J. Phys. Chem. C*, 2012, **116**, 9000–9008.
- 6 S. P. Wang, S. Westcott and W. Chen, *J. Phys. Chem. B*, 2002, **106**, 11203–11209.
- 7 F. Vetrone, R. Naccache, A. Zamarron, A. J. de la Fuente, F. Sanz-Rodriguez, L. M. Maestro, E. M. Rodriguez, D. Jaque, J. G. Sole and J. A. Capobianco, *ACS Nano*, 2010, **4**, 3254–3258.
- 8 L. M. Maestro, C. Jacinto, U. R. Silva, F. Vetrone, J. A. Capobianco, D. Jaque and J. G. Sole, *Small*, 2011, **7**, 1774–1778.
- 9 Y. H. Gao and Y. Bando, *Nature*, 2002, **415**, 599.
- 10 Y. B. Li, Y. Bando, D. Golberg and Z. W. Liu, *Appl. Phys. Lett.*, 2003, **83**, 999–1001.
- 11 M. G. Cerruti, M. Sauthier, D. Leonard, D. Liu, G. Duscher, D. L. Feldheim and S. Franzen, *Anal. Chem.*, 2006, **78**, 3282–3288.
- 12 D. R. Schmidt, C. S. Yung and A. N. Cleland, *Appl. Phys. Lett.*, 2003, **83**, 1002–1004.
- 13 E. Shapira, D. Marchak, A. Tsukernik and Y. Selzer, *Nanotechnology*, 2008, **19**, 125501.
- 14 L. Rayleigh, *Proc. London Math. Soc.*, 1878, **10**, 4.
- 15 Y. Bisrat, Z. P. Luo, D. Davis and D. Lagoudas, *Nanotechnology*, 2007, **18**, 395601.
- 16 <http://www.indium.com/solders>.
- 17 F. A. Nichols and W. W. Mullins, *Trans. Metall. Soc. AIME*, 1965, **233**, 1840.
- 18 P. H. Chen, C. H. Hsieh, S. Y. Chen, C. H. Wu, Y. J. Wu, L. J. Chou and L. J. Chen, *Nano Lett.*, 2010, **10**, 3267–3271.
- 19 L. F. Liu, W. Lee, R. Scholz, E. Pippel and U. Gosele, *Angew. Chem., Int. Ed.*, 2008, **47**, 7004–7008.
- 20 M. E. Toimil-Molares, A. G. Balogh, T. W. Cornelius, R. Neumann and C. Trautmann, *Appl. Phys. Lett.*, 2004, **85**, 5337–5339.
- 21 Y. Qin, S. M. Lee, A. Pan, U. Gosele and M. Knez, *Nano Lett.*, 2008, **8**, 114–118.
- 22 J. Lian, L. M. Wang, X. C. Sun, Q. K. Yu and R. C. Ewing, *Nano Lett.*, 2006, **6**, 1047–1052.
- 23 S. Karim, M. E. Toimil-Molares, A. G. Balogh, W. Ensinger, T. W. Cornelius, E. U. Khan and R. Neumann, *Nanotechnology*, 2006, **17**, 5954–5959.
- 24 H. S. Shin, J. Yu and J. Y. Song, *Appl. Phys. Lett.*, 2007, **91**, 173106.
- 25 V. P. Parkhutik and V. I. Shershulsky, *J. Phys. D: Appl. Phys.*, 1992, **25**, 1258–1263.
- 26 <http://www.shockwatch.com/products/temperature-indicators/warmmark2/>.